Wettability of Silicon Carbide by CaO-SiO_2 Slags

JAFAR SAFARIAN and MERETE TANGSTAD

The wettability of silicon carbide by liquid CaO-SiO_2 slags that contain 47 to 60 wt pct SiO_2 was studied using the sessile drop wettability technique. The experiments were carried out in Ar and CO atmospheres. A small piece of slag was melted on SiC substrates under different heating regimes up to 1600 °C. It was found that the wetting is not significantly dependent on the temperature and the heating rate. However, the wettability is relatively high, and the wetting is higher for slags that contain lower SiO_2 concentrations. Moreover, the wettability between the slags and SiC is dependent on the gas phase composition, and it is higher in Ar than that in CO. When the SiO_2 concentration changes from 47 pct wt to 60 pct wt, the wetting angle changes from 20 deg to 73 deg in Ar and from 58 deg to 87 deg in a CO atmosphere. The formation and bursting of gas bubbles also was observed after some contact time, which indicates that the wetting system is a reactive type. However, microscopic studies indicated that no metal phase exists at the slag/silicon–carbide interface. Therefore, it was concluded that chemical reactions between the slag and SiC take place and that SiO_2 is slowly reduced to form CO and SiO gases. Based on the experimental data, the dependence of the Girifalco–Good coefficient on the slag composition and the relationship between the interfacial tension of CaO-SiO_2 slags and SiC also were estimated.

DOI: 10.1007/s11663-009-9292-5

I. INTRODUCTION

INTERFACIAL properties at the solid–liquid interface play an important role in many metallurgical processes. The degree of wetting a solid by a liquid in a solid–liquid–gas, three-phase system is characterized by the conditions of thermodynamic equilibrium. The profile adopted by a liquid drop resting in equilibrium on a flat horizontal surface is governed by the balance between surface and gravitational forces (Figure 1). The relationship between the contact angle and the respective interfacial tensions acting at point A of three-phase contact is given in the Young equation,[1] which is as follows:

$$(\gamma_{SG} - \gamma_{LS}) = \gamma_{LG} \times \cos\theta \qquad [1]$$

where θ is the contact angle and γ_{LG}, γ_{LS}, and γ_{SG} are the liquid/gas, liquid/solid, and solid/gas interfacial tensions, respectively. When a reaction occurs at the interface, the free energy change per unit area per unit time also enhances wetting. In this case, the Young equation [1] should be corrected for this driving force. According to Laurent,[2] the smallest contact angle possible in a reactive system is given as follows:

$$\cos\theta_{min} = \cos\theta_0 - \frac{\Delta\gamma_r}{\gamma_{LG}} - \frac{\Delta G_r}{\gamma_{LG}} \qquad [2]$$

Here, θ_0 is the contact angle of the liquid on the substrate in the absence of any reaction. $\Delta\gamma_r$ takes into account the change in interfacial energies brought about by the interfacial reaction, and ΔG_r is the change in free energy per unit area released by the reaction in the immediate vicinity of the liquid/substrate interface. In general, ΔG_r is one of the major factors that governs wetting in the reactive system. However, it is difficult to determine this value quantitatively from experiments or from theoretical calculations. In reality, the difficulty remains in correlating the time-dependent interfacial reaction with the kinetics of wetting.

In many metallurgical processes, silicon carbide (SiC) is in contact with molten phases. For instance, more than 65 pct of the industrialized world's iron blast furnaces use SiC bricks as the lining materials.[3] Silicon carbide also has contact with molten aluminum and cryolite in electrolytic reduction cells for the production of aluminum, in which SiC is used as the sidewall lining.[4] In the directional solidification of silicon, which is used to produce silicon feedstock for solar cells, when carbon exceeds its solubility limit in silicon, SiC particles are produced and dispersed throughout the melt.[5] In the present study, the contact between silicon carbide and CaO-SiO_2 melts is investigated.

The surface tension of CaO-SiO_2 slags has been measured in several studies. The dependence of slag surface tension on the temperature is small.[6–10] For instance, on the one hand, the surface tension of a slag with 0.44 molar fraction of SiO_2 in argon decreases from 455 mNm^{-1} to 445 mNm^{-1} with increasing temperature from 1470 °C to 1600 °C.[10] On the other hand, the dependence of surface tension on temperature varies in regard to the gas phase. The slag surface tension decreases slowly with an increasing temperature in

JAFAR SAFARIAN, Researcher, and MERETE TANGSTAD, Professor, are with the Norwegian University of Science and Technology, Alfred Getz Vei 2, 7491, Trondheim, Norway. Contact e-mail: Jafar.Safarian@material.ntnu.no and Merete.Tangstad@material.ntnu.no.

Manuscript submitted February 11, 2009.
Article published online September 1, 2009.

argon, whereas it increases minimally with an increasing temperature in oxygen.[10] Considering the slag with 0.44 molar fraction of SiO_2, its surface tension at 1550 °C in oxygen is 425 mNm^{-1}, whereas it is 450 mNm^{-1} in argon. The surface tension of $CaO\text{-}SiO_2$ slags is mainly dependent on the slag chemical composition, and it increases with a decline in the SiO_2 concentration. For instance, surface tensions of slags containing 0.415 and 0.634 molar fraction of SiO_2 at 1600 °C are 477 mNm^{-1} and 380 mNm^{-1}, respectively.[9] The relationship between the surface tension and the composition of $CaO\text{-}SiO_2$ slags will be described later.

II. METHODOLOGY

The contact of various $CaO\text{-}SiO_2$ compositions with SiC at elevated temperatures was investigated using the sessile drop wettability technique as described in the next section.

A. *Experimental Setup and Conditions*

A horizontal tube furnace was used to study the wetting properties in the sessile drop method. A schematic diagram of the experimental setup is shown in Figure 2. The sample is located in the center of the heating element, which is in the middle of the chamber. All heated furnace parts, which include the element and heat shields, are constructed of graphite, which allows for both extremely fast and slow heating or cooling rates. The temperature of the furnace is controlled using a Keller (GMBH, Ibbenduren, Germany) PZ40 two-color pyrometer that operates from 900 °C to 2400 °C

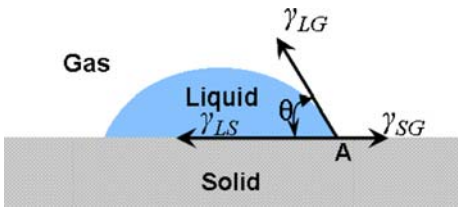

Fig. 1—The relations at equilibrium between the respective surface and interfacial-tensions and the contact angle θ in wetting condition.

focused on the edge of the graphite sample holder. A fire-wire digital video camera (Sony XCD-SX910CR, Sony Corporation, Tokyo, Japan) with a telecentric lens (Navitar 1-50993D, Navitar Inc., New York, NY) is used to record images from the sample at 960 × 1280 pixels. The telecentric lens is especially suitable for this type of measurement, with a 12 times zoom that allows for an image size from 50 to 4 mm across the frame, which at maximum magnification is equivalent to 3 μm per pixel. A Cambridge Sensotec Rapidox 2100 (St. Ives, UK) (with a range from 10^{-17} ppm to 100 pct O_2) was used to measure the partial pressure of oxygen continually in the gas outlet during the experiments.

The furnace was designed to study the contact properties, the interaction between a small liquid sample, and a solid substrate with 10 mm diameter and 2 to 5 mm height. The liquid drop must be small enough to sit on top of the substrate without touching the edges. In this study, a piece of slag with 15 ± 1-mg mass was added on SiC substrate. The furnace chamber was evacuated initially and then filled with the required atmosphere. Pure argon (99.9999 pct) was used as the gas phase in most experiments, and a few experiments were carried out in a CO atmosphere.

Two heating regimes were used for the experiments. For regime I, the furnace was heated to 900 °C in approximately 10 minutes and then to 1500 °C at 50 °C/min. The sample then was heated with the rate of 20 °C/min to 1550 °C and then to 1600 °C with holding times for 15 minutes. Finally, the sample was cooled rapidly to room temperature. For regime II, the furnace was heated to 900 °C, similar to regime I. Then, it was heated with 120 °C/min to 1600 °C, was held for 15 minutes, and finally was followed by rapid cooling to room temperature.

The time of the completely liquid drop formation was considered as the initial contact time. Some photos taken from the samples were used to measure the contact angle between the SiC and slag droplets. The samples examined with the slow heating rate in regime I also were mounted, and cross sections of them were prepared. These cross sections were used to determine the chemical composition of slags and to study the interfacial area between SiC and slags by the Electron Probe Micro Analyser (JEOL JXA-8500F Hyperprobe, JEOL Ltd., Tokyo, Japan).

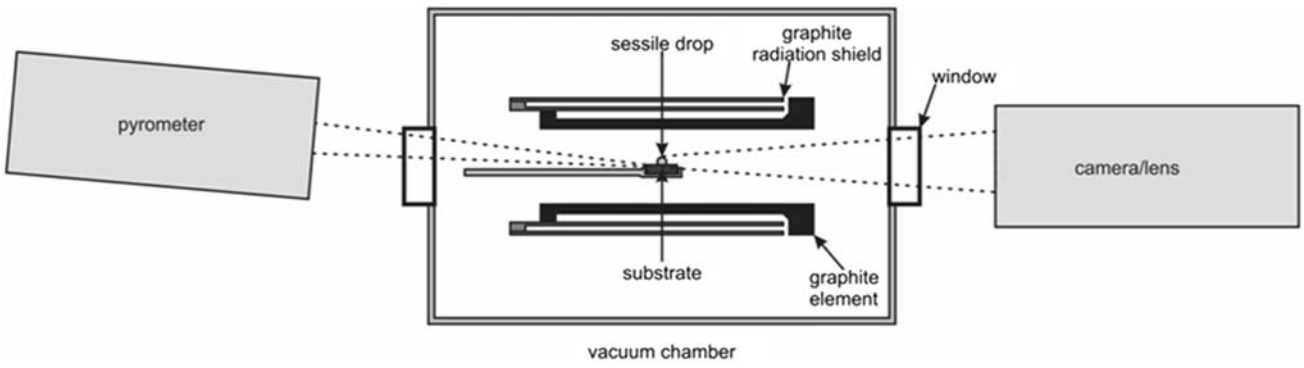

Fig. 2—Schematic diagram of the experimental setup.

B. *Materials*

1. *Slag*

In the present study, $CaO\text{-}SiO_2$ slags that contained 47 pct, 50 pct, 55 pct, and 60 pct SiO_2 were used, which are called slags A, B, C, and D, respectively. These slags were prepared by mixing pure oxides of calcium and silicon and then melting them in graphite crucible in an induction furnace. The obtained slags then were casted and crushed down. The compositions of the prepared slags are shown on the $CaO\text{-}SiO_2$ phase diagram in Figure 3.[11]

2. *Silicon carbide*

Two forms of SiC substrates were used. First, a flat surface of SiC powder was prepared. In this case, the SiC powder was pressed using 63.7-kg/cm^2 pressure in a small graphite crucible with an 8 mm inside diameter, a 3 mm height, and a 1 mm depth. It was found that a substrate made of SiC particles is not proper for measuring the wettability parameters, which will be discussed in Section III–A. Therefore, a single crystal substrate of SiC was used. In this case, single crystals from a commercially produced SiC bunch were separated, and they were polished by diamond disk to make flat SiC plates with approximately 1 mm thickness. It is worth noting that the structure of SiC single crystal was studied by X-ray diffraction (XRD) with Copper target and by changing the diffraction angle between 20 and 60 deg. The silicon carbide was characterized as α-SiC that contains mainly Moissanite-6H with some Moissanite 4H and possibly some Moissanite-3C.

III. RESULTS AND DISCUSSION

The obtained results from the wettability experiments on SiC powder and single crystal substrates are presented and discussed in this section.

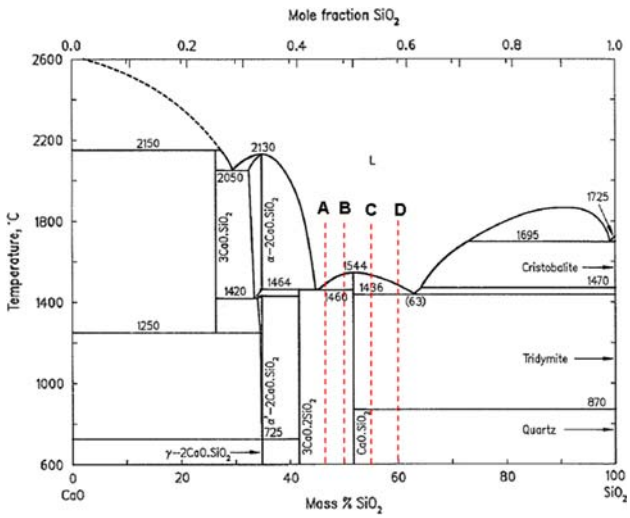

Fig. 3—The $CaO\text{-}SiO_2$ phase diagram[11] and the composition of the prepared slags.

A. *Wettability of Sic Powder*

The wettability of SiC powder substrate with slags B and D was investigated in Ar with the heating regime I. It was observed that slag B starts to melt at 1585 °C, whereas slag D starts to melt at 1478 °C. Observing a lower melting point for slag D than for slag B agrees with the melting point difference in the phase diagram (Figure 3). The higher melting point for slag B, which was greater than the observed melting point in the phase diagram (1540 °C), can be related to the photos taken from one side of the particle. It also may be related to the heat transfer from the substrate to the slag particle. In this case, the contact between the slag piece and the substrate—where heat is transferred to the slag—is important, because the sample melts faster when higher contact areas exist.

It was observed that the liquid slag droplet is stable for a short time on the substrate and then it disappears through slag penetration into the SiC substrate. The lifetime of the droplet was 5 seconds for slag B and approximately 3 minutes for slag D as illustrated on the sample temperature profile in Figure 4. The shorter lifetime of the slag B droplet compared with the slag D droplet may be related to the better wettability of SiC by slag B. This advantage can be found in the changes of the contact angle for both slags as shown in Figure 5. Better wetting of SiC by slag B creates a faster flow between the SiC particles so that the droplet disappeared in 5 seconds as shown in Figure 6.

Considering good wetting of SiC by slags B and D as well as the rapid changes of the contact angle, it is difficult to determine properly the contact angle. As mentioned, the observed rapid change in the contact angle is related mainly to the mass transport of liquid slag into the SiC substrate. If a bulk substrate of SiC is used instead of SiC powder, then a much slower slag penetration, or no penetration, is expected. Hence, the wettability of SiC single crystal by the slags was studied.

B. *Wettability of SiC Single Crystal*

The results of the wettability of SiC single crystal by slags A, B, C, and D in an Ar atmosphere and by slags A

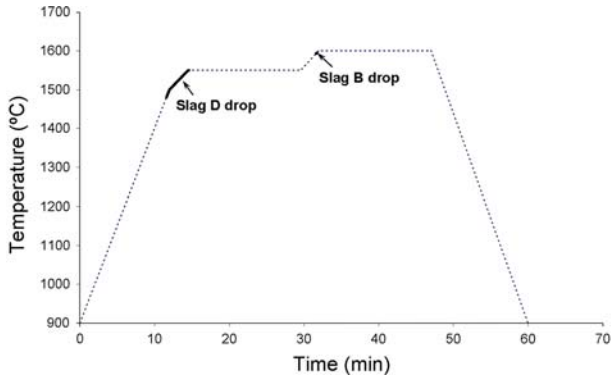

Fig. 4—The stable range of the droplets of slags B and D on SiC powder substrate on the sample heating regime.

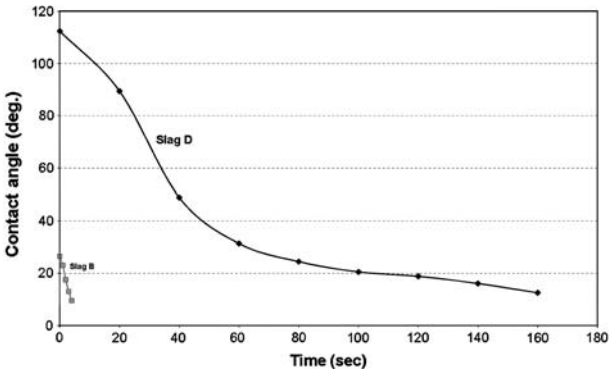

Fig. 5—The changes of the contact angle between slag drops and SiC powder substrate after the formation of a complete liquid slag.

and D in a CO atmosphere are described in the following sections.

1. *Wettability in Ar*

For the experiments in heating regime I, it was observed that slags A through D start to melt at 1580 °C, 1567 °C, 1530 °C, and 1493 °C, respectively. These melting points are equal to or above the melting point of these slags on the phase diagram (Figure 3). This inconsistency may be caused by the continuous heating of the samples, the sample observing angle, personal errors, or the heat transferred from the substrate to the slag particle as described earlier. The observed melting points for slags B and D during the experiments on SiC single crystal were different from the melting points observed during the experiments on

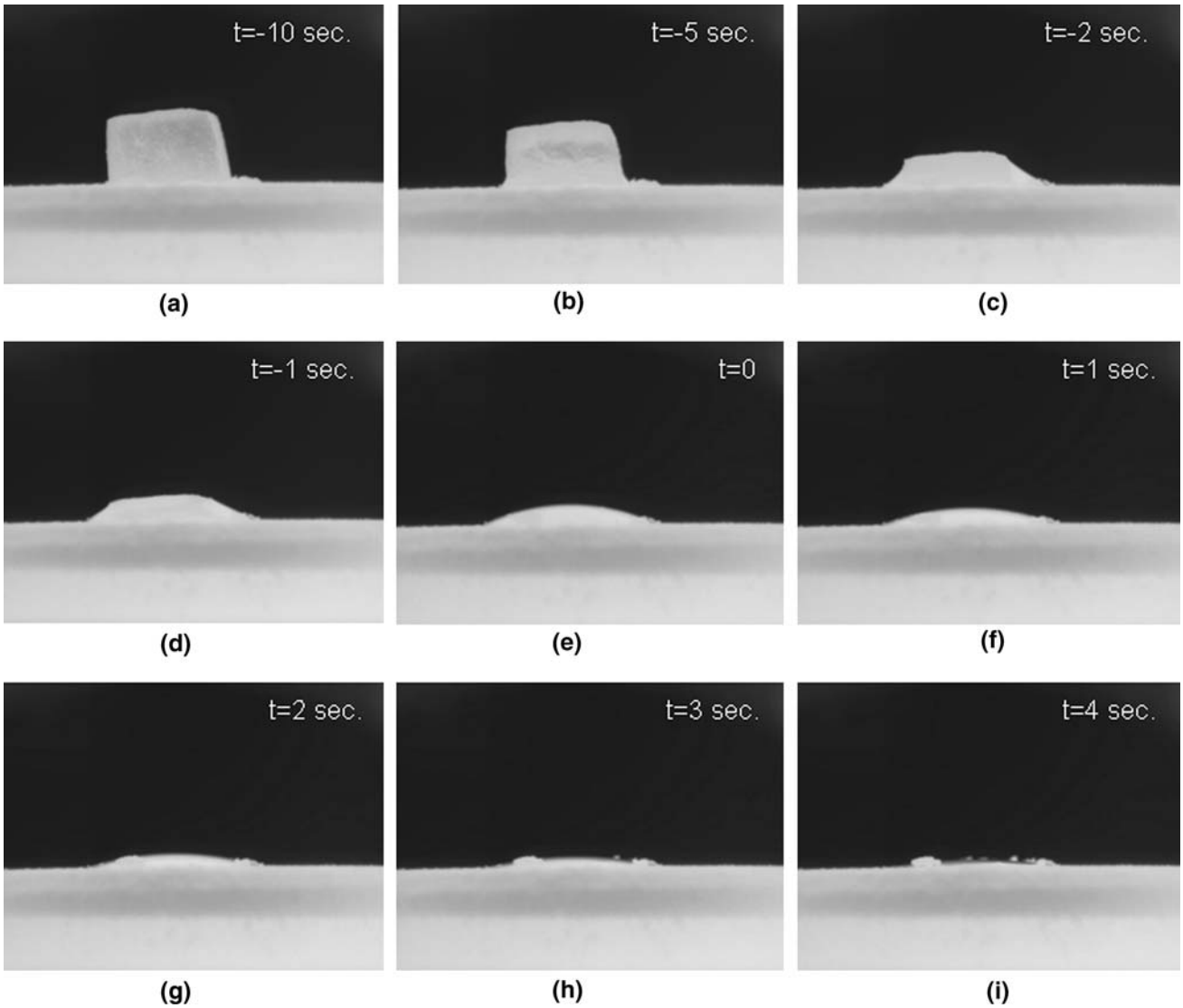

Fig. 6—The contact of slag B (CaO-50 pct SiO_2) with SiC powder substrate. Images (*a*) to (*d*): before complete melting, image (*e*): completely liquid drop formation, and images (*f*) to (*i*): second by second after drop formation.

Table I. The Temperature Range and Duration of Observing Single-Phase Liquid Drop of Slag on SiC Single Crystal

	Heating Regime I		Heating Regime II	
Slag	Temperature Range	Duration	Temperature Range	Duration
A	1600 °C–1600 °C	5 min	1600 °C–1600 °C	0.9 min
B	1600 °C–1600 °C	4 min	1580 °C–1600 °C	3.2 min
C	1530 °C–1557 °C	3.3 min	1530 °C–1600 °C	11.45 min
D	1500 °C–1550 °C	11.8 min	1500 °C–1600 °C	2.8 min

SiC powder substrate. This may be related to the observations, the shape of the solid slag particle, or the heat transfer to the particle through the substrate. The melted slag appeared to be a completely liquid drop some time after it started to melt. The slag was drop-shaped for a length of time, and then, gas bubbles started to appear. The period of time it took for the slag to melt completely and for bubbles to appear as well as the correspondent temperature ranges are presented for all slags in Table I.

For the experiments in heating regime II, it was observed that slags A through D started to melt at 1590 °C, 1580 °C, 1530 °C, and 1500 °C, respectively. These melting points again are above the melting point of the slags on the phase diagram. However, they are similar to the observed melting points in slow heating rate experiments, although slightly higher. The melted slag again was a complete liquid drop some time after melting and remained so for an extended period of time (Table I) before bubble formation occurred.

The changes of the contact angle between the slags and the SiC for both slow and rapid heating rates are shown in Figure 7. As we observe in the figure, the wetting of SiC is dependent on the slag chemical composition. Obviously, wetting is better for lower SiO_2 contents. As also shown, the contact angle for the slags containing 50 pct and 47 pct SiO_2 is relatively low and with similar trend, whereas for slags containing 55 pct and 60 pct SiO_2 is higher and initially decreases fast and then levels off. Figure 7 indicates that the contact angle for slags with higher SiO_2 concentrations is always larger except for slag D in Figure 7(b). Heating rate and temperature have no significant effect on the contact angle as observed in Figure 7, whereas the effect of slag chemical composition is considerable. This observation is in agreement with the dependence of the surface tension of $CaO\text{-}SiO_2$ slags with the temperature and slag chemical composition as described earlier.

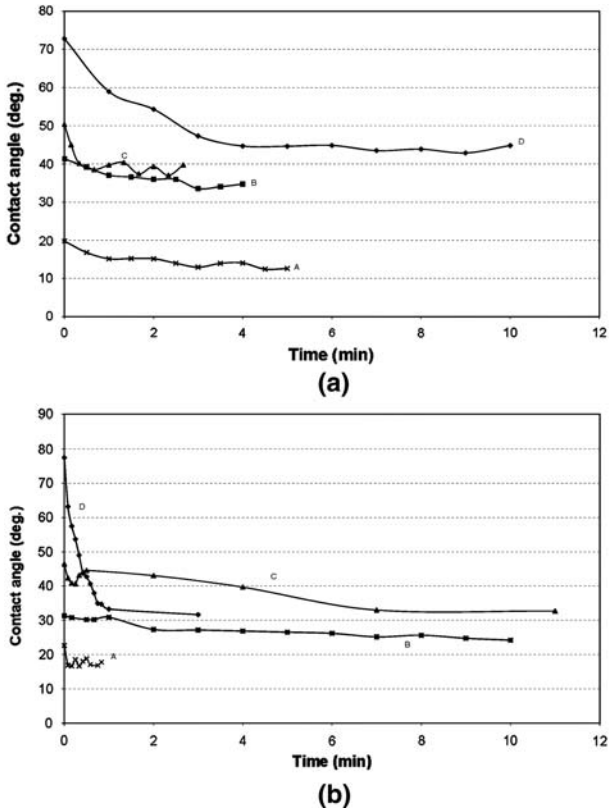

Fig. 7—The changes in the contact angle between slag drops and SiC single crystal substrate after the formation of a complete liquid slag in slow (*a*) and rapid (*b*) heating regimes.

2. *Wettability in CO*

In principle, the type of gas phase in the sessile drop method can affect the wetting properties by affecting the liquid/gas and solid/gas interfacial tensions. To study the effect of the gas phase on the wettability of SiC by $CaO\text{-}SiO_2$ slags, the wettability experiments were carried out in a CO atmosphere for slags A and D. In this case, the experiments were carried out with the heating regime II and used SiC single crystal as the substrate.

It was found that the contact angle is always larger in CO gas than in Ar gas as shown in Figure 8. However, the contact angle changes in a CO atmosphere are fewer than the contact angle changes in an Ar atmosphere. It also was observed that bubble formation and bubble bursting in a CO atmosphere is much less than that in an Ar atmosphere, so it was possible to measure the contact angle in longer contact times as observed in Figure 8.

The larger contact angle in a CO atmosphere than in an Ar atmosphere may be related to the lower oxygen partial pressures when CO is used. The measured oxygen partial pressures in the gas outlet from the furnace chamber indicated that the oxygen partial pressure for the experiments in CO are around 10 times lower than the oxygen partial pressure for the experiments in Ar $\left(p_{O_2 \text{ in AR}} = 1 \times 10^{-23}\text{atm}\right)$. Lower oxygen partial pressure may increase the slag surface tension and, therefore, contact angle as mentioned by Sharma and Philbrook.[8]

C. *Theoretical Aspects of SiC Contact with the Slag*

The initial contact angle after the melting of slag and the final contact angle before bubble formation are shown in Figure 9 with corresponding sample temperatures. As we observe, a range of contact angle exists for each slag composition, and this range increases with increasing SiO_2 concentration. The bubble formation and bubble bursting also are observed later for higher SiO_2 concentrations. The bubbles indicate that we face a reactive system, and chemical reactions take place at the slag/SiC interfacial area. Assuming that the spread of slag on the substrate is caused by these chemical reactions, the initial contact angle between the slags and SiC can be considered as the static contact angle. This assumption is fairly reasonable because contact between the reactants is necessary prior to the chemical reactions. The relationship between the initial contact angles and SiO_2 concentrations for both Ar and CO atmospheres is shown in Figure 9 by the dashed lines.

It is difficult to calculate the contact angle between the CaO-SiO_2 slags and the SiC substrate because of the lack of experimental data in literature as well as the accuracy of the databases of the commercial chemical and thermodynamic software. However, this contact can be studied with regard to the developed theories for the contact of liquids and solids. An equation that relates the free energies of cohesion for separate phases to the free energy of adhesion, and hence the surface tensions to the interfacial tensions, was proposed by Girifalco and Good[12]:

$$2\Phi\sqrt{\gamma_{SG}\gamma_{LG}} = \gamma_{SG} + \gamma_{LG} - \gamma_{LS} \quad [3]$$

The proportionality factor Φ is somewhat a semiempirical factor and varies generally in the range between 0.32 and 1.15. The contact angle between solid and liquid can be calculated from Eqs. [1] and [3] as follows[13]:

$$\cos\theta = 2\Phi\sqrt{\frac{\gamma_{SG}}{\gamma_{LG}}} - 1 \quad [4]$$

The surface energy of SiC structures has been estimated according to the simple broken bond model of Skapski.[14] This model predicts a surface energy value of 1450 mNm^{-1} for the (0001) face of hexagonal α-SiC. This value is the same for the (111) face of cubic SiC, because they have the same atomic structure. It is worth noting that this value is lower but still close to the value of 1767 mNm^{-1} that was estimated by Takai *et al.*[15] using Monte Carlo simulations for a relaxed (111) face of cubic SiC. Unfortunately, no measured data about the surface energy of crystal faces of hexagonal α-SiC was found in the literature. Such data can help us obtain the average surface energy of the crystal faces and apply it for more representative calculations.

It was mentioned that the surface tension of CaO-SiO_2 slags mainly is dependent on the slag chemical composition and not on the temperature. The relationship between slag surface tension and SiO_2 concentration is shown in Figure 10 and is based on the surface tension measurements in an Ar atmosphere.[8–10] As observed, the slag surface tension decreases linearly with an increasing SiO_2 concentration, which is shown as follows:

$$\gamma_{LG} = 681.58 - 474.15X_{SiO_2} \quad [5]$$

The contact angle between CaO-SiO_2 slags and SiC substrate was calculated as a function of SiO_2

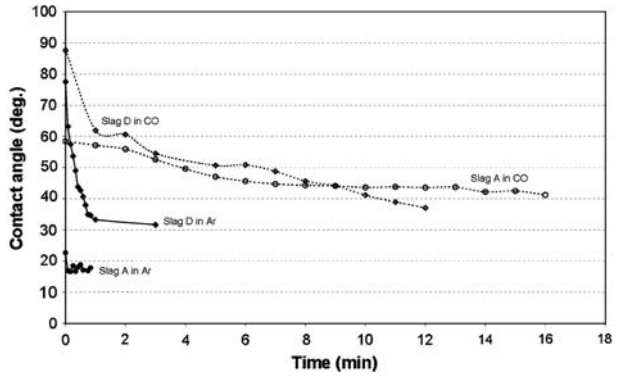

Fig. 8—The changes in the contact angle between slags A and D and SiC single crystal substrate in Ar and CO atmospheres (rapid heating regime II).

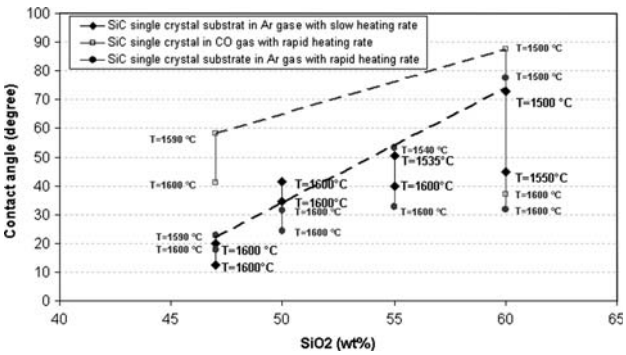

Fig. 9—The changes in the measured contact angle between slag and SiC substrates in regard to the temperature of samples (symbols), and the fitted line to the initial contact angles in Ar and CO atmospheres (dashed lines).

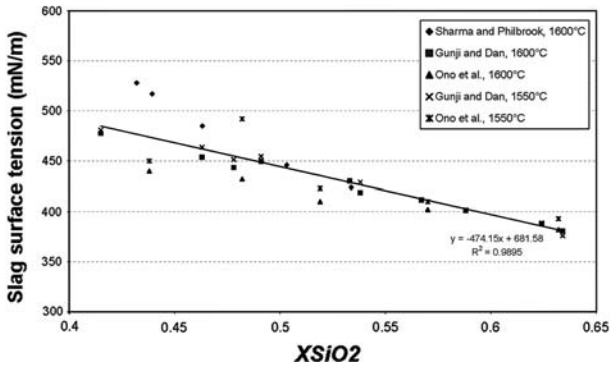

Fig. 10—The relationship between the surface tension of CaO-SiO_2 slags and the slag composition based on the experimental measurements in Ar atmosphere.

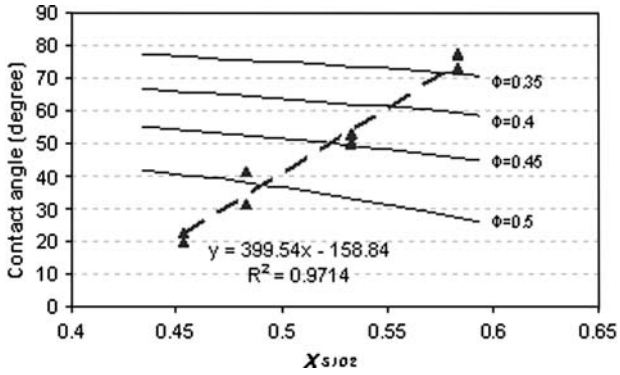

Fig. 11—The relation between the contact angle and the SiO_2 concentration; theoretical calculations for fixed Φ values (solid curves) and measured (dashed line).

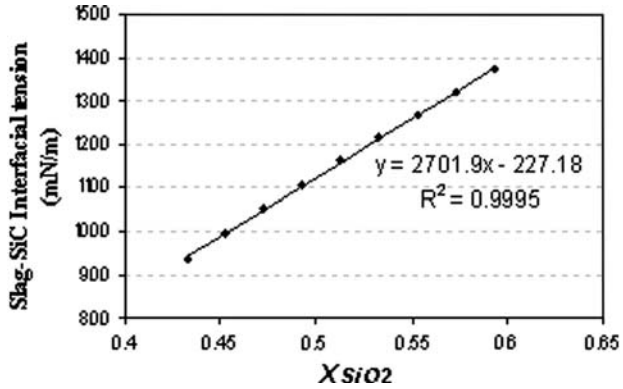

Fig. 12—The slag/SiC interfacial tension dependence on slag composition.

concentration using Eqs. [4] and [5] and assuming $\gamma_{SG} = 1450\ mNm^{-1}$. The results for various Φ values are illustrated in Figure 11 by solid curves. As shown, the calculated contact angle is dependent on the Φ value, and it is larger for smaller Φ values. The relationship between the measured contact angles in Ar and the slag composition also are represented in Figure 11. Considering the crossover points of the fitted line to the measured contact angles (dashed line) and the theoretical calculated curves, the dependency of Φ to the slag chemical composition may be obtained as follows:

$$\Phi = 1.35 - 1.74X_{SiO_2} \quad [6]$$

Considering Eqs. [5] and [6] as well as $\gamma_{SG} = 1450\ mNm^{-1}$, the interfacial tension between the slag and SiC was calculated from Eq. [3] for various SiO_2 concentrations as shown in Figure 12. Obviously, a fair linear relationship exists between the interfacial tension and the composition changes:

$$\gamma_{LS} = 2701.9X_{SiO_2} - 227.18 \quad [7]$$

D. *Reactions in the System*

Using wavelength dispersive spectroscopy (WDS) by EPMA to analyze the slags contact with SiC single crystal in Ar indicated that the chemical composition of the slags is not far from that of the original slags. The SiO_2 content of slags A, B, C, and D was 48.6 pct, 49.6 pct, 54.7 pct, and 59.7 pct, respectively. These results may indicate that the extent of SiO_2 reduction from the slags by SiC, which is the reason for the bubble formation, is not substantial within the applied contact times.

The interfacial area between the slags and SiC single crystal are shown in Figure 13. As is shown, no penetration occurs of slag into the SiC single crystal. This observation may prove that the observed penetration of slag in SiC powder substrate only is caused by the high wetting and not by the chemical reactions. Many cracks also occur in the solidified slags, which are related to the changes in the slag structure during solidification. Moreover, the amount of the bubbles trapped in the solidified slag increases with an increase in the SiO_2 concentration, as observed for slags C and D in Figure 13. This result may indicate that the gas holdup of CaO-SiO_2 slags increases with an increase in the SiO_2 concentration.

Inspecting the interfacial area between the SiC and slags indicated that no metal phase exists at the interface, which signifies that the reactions in the system do not lead to the formation of silicon metal. This indication may be because silicon production requires low activities of silicon, which is not fulfilled through the contact of slag and SiC. According to these observations, therefore, it can be suggested that SiO_2 slag reacts with SiC to form gaseous products, which are shown as follows:

$$2(SiO_2) + SiC = 3SiO\,(g) + CO\,(g) \quad [8]$$

Considering unit activity for SiC, $p_{SiO} + p_{CO} = 1$ and the Gibbs free energy of the above reaction (ΔG^0), the partial pressure of SiO, $p_{SiO,}$ at equilibrium in a CO atmosphere can be determined by the equation:

$$p_{SiO}^3(1 - p_{SiO}) = \exp\left(-\frac{\Delta G^0}{RT}\right) \times a_{SiO_2} \quad [9]$$

Quartic function Eq. [9] was solved by Ferrari's solution method for given SiO_2 activities and various temperatures, and the results are illustrated in Figure 14. ΔG^0 for various temperatures was calculated by HSC Chemistry version 4.1 (Outokumpu Research Oy, Finland). As is shown, the equilibrium partial pressure of SiO increases with increasing SiO_2 activity and temperature.

The activity of SiO_2 in slag is significantly dependent on the chemical composition. For instance, Chipman[16] measured $a_{SiO_2} = 0.05$ for a molar fraction of SiO_2 equal to 0.46 at 1600 °C, whereas Kay and Taylor[17] measured $a_{SiO_2} = 0.16$ for a molar fraction of SiO_2 equal to 0.48 at 1550 °C. The activity of SiO_2 increases with an increase in the SiO_2 concentration, and it is approximately unity for molar fractions of SiO_2 equal to 0.63.[18]

In regard to the SiO_2 activities in the slags and the corresponding high-equilibrium partial pressures of SiO gas in the system, chemical reaction [8] proceeds at the

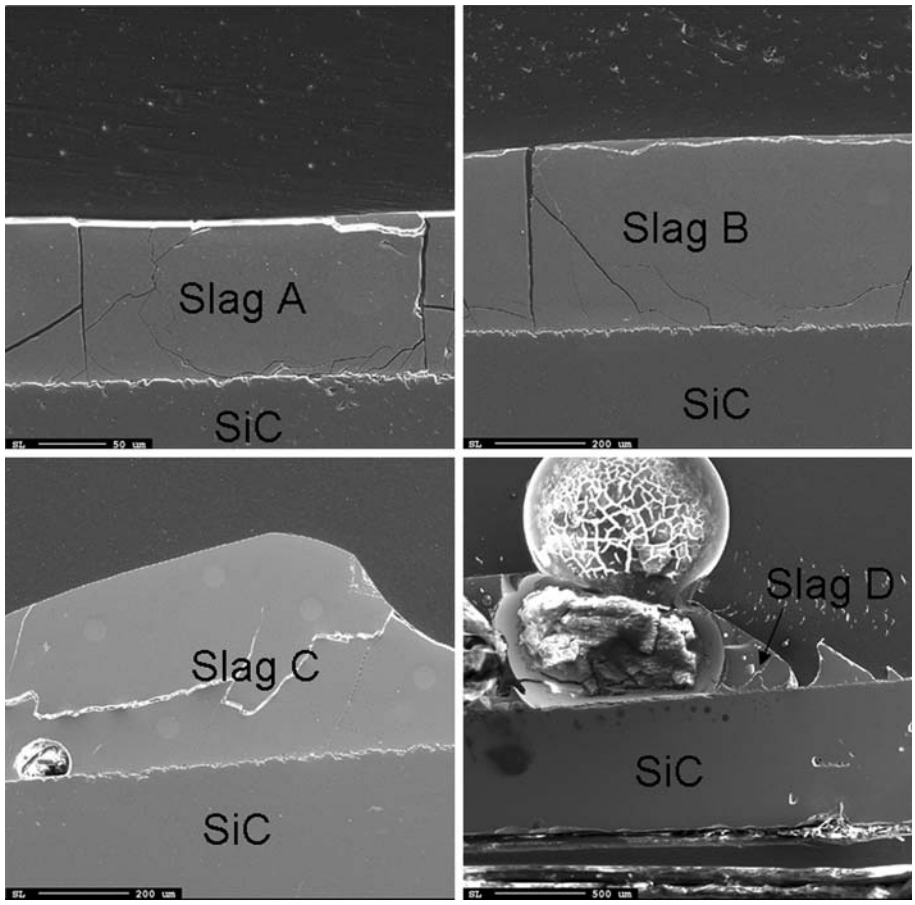

Fig. 13—The cross sections of the solidified slags on SiC single crystal substrate.

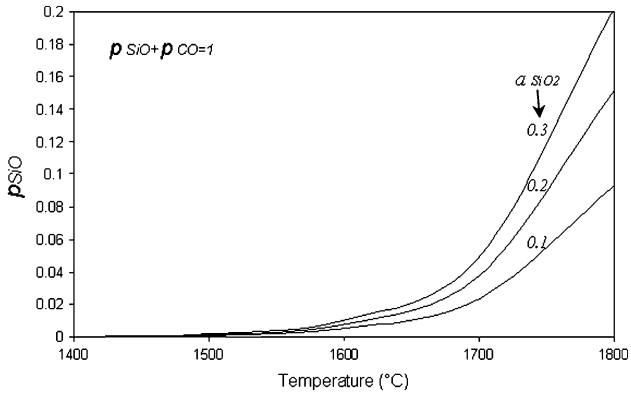

Fig. 14—The relationship between the equilibrium partial pressure of SiO gas with temperature for various SiO_2 activities (reaction [8]).

slag–silicon carbide interfacial area. The continuous flows of pure Ar and CO in the furnace chamber maintain the small SiO partial pressures, so the chemical reaction is always far from the equilibrium in the applied reaction. It is worth noting that for the case of using CO gas, reaction [8] takes place slower than in Ar because of the smaller driving force for the reaction. This observation occurred in the experiments with much less bubble bursting from the slag surface in CO atmosphere.

IV. CONCLUSIONS

The wettability of SiC powder and SiC single crystal by CaO-SiO_2 slags was investigated by the sessile drop wettability technique, and the results are as follows:

1. The wetting of SiC by CaO-SiO_2 slags is relatively high. The CaO-SiO_2 slag penetrates to the SiC powder substrate because of high wetting, whereas no penetration occurs when SiC-single crystal is used.
2. The contact angle between CaO-SiO_2 slags and SiC mainly is dependent on slag chemical composition and atmosphere, whereas the heating rate (temperature) has no significant effect.
3. The wetting decreases with increasing SiO_2 content. The wetting angle changes from 20 deg to 73 deg when SiO_2 concentration changes from 47 pct to 60 pct in Ar atmosphere.
4. The wetting in a CO atmosphere is less than that in Ar atmosphere. The wetting angle changes from 58 deg to 87 deg when SiO_2 concentration changes from 47 pct to 60 pct in CO atmosphere.
5. Based on the available thermodynamic databases, it is difficult to calculate the accurate contact angle between SiC and CaO-SiO_2 slags.
6. Bubble growth and bubble bursting from the slag droplet take place through the SiO_2 reduction by SiC substrate. According to the microscopic studies, the

reactions in the system do not lead to the silicon metal formation and only CO and SiO gases are formed.

7. Based on the Girifalco–Good theory, the relationship between the slag/SiC interfacial tension and slag composition was calculated as follows: $\gamma_{LS} = 2701.9X_{SiO_2} - 227.18$.

OPEN ACCESS

REFERENCES

1. T. Young: *Phil. Trans. R. Soc. Lond.*, 1805, vol. 95, pp. 65–87.
2. V. Laurent: Ph.D. Dissertation, Institut National Polytechnique de Grenoble, France, 1988.
3. G.X. Wang, P.E.I. Benyan, and J.D. Lister: *ISIJ Int.*, 1998, vol. 38 (12), pp. 1326–31.
4. E. Skybakmoen, H. Gudbrandsen, and L.I. Stoen: *Proc. 12th TMS Annual Meeting*, 2003, pp. 215–22.
5. L. Liu, S. Nakano, and K. Kakimoto: *J. Crystal Growth*, 2008, vol. 310, pp. 2192–97.
6. K. Mukai and T. Ishikawa: *Nippon Kinzoku Gakkaishi*, 1981, vol. 45 (2), p. 147.
7. T.B. King: *J. Soc. Glass Technol.*, 1951, vol. 35, p. 241.
8. S.K. Sharma and W.O. Philbrook: *Proc. Int. Conf. Sci. Tech. Iron Steel*, 1970.
9. K. Gunji and T. Dan: *Trans. ISIJ*, 1974, vol. 14, p. 162.
10. K. Ono, K. Gunji, and T. Araki: *Nippon Kinzoku Gakkhai*, 1969, vol. 33 (3), p. 299.
11. M. Allibert, R. Para, C. Saint-Jours, and M. Tmar: *Slag Atlas*, 2nd ed., Verlag Stahleisen GmbH, Dusseldorf, Germany, 1995, pp. 225–55.
12. L.A. Girifalco and R.J. Good: *J. Phys. Chem.*, 1957, vol. 61 (7), p. 904.
13. L.A. Girifalco and R.J. Good: *J. Phys. Chem.*, 1960, vol. 64 (5), p. 561.
14. N. Eustathopoulos, M.G. Nicholas, and B. Drevet: *Wettability at High Temperatures*, Pergamon, Oxford, UK, 1999.
15. T. Takai, T. Halicioglu, and W.A. Tiller: *Surf. Sci.*, 1985, vol. 164, p. 341.
16. J. Chipman: *Physical Chemistry of Process Metallurgy*, part 1, Interscience, New York, NY, 1961.
17. D.A.R. Kay and J. Taylor: *Trans. Faraday Soc.*, 1960, vol. 56, pp. 1372–86.
18. M. Kowalski, P.J. Spencer, and D. Neuschutz: *Slag Atlas*, 2nd ed., Verlag Stahleisen, Dusseldorf, Germany, 1995, p. 63.